LTE-compatible 5G PHY based on Generalized Frequency Division Multiplexing

Ivan Gaspar†, Luciano Mendes*, Maximilian Matthé†, Nicola Michailow†, Andreas Festag†, Gerhard Fettweis†

† Vodafone Chair Mobile Communication Systems, Technische Universität Dresden, Germany
* Inatel, Sta. Rita do Sapucai, MG, Brazil
{ivan.gaspar,luciano.mendes,maximilian.matthe,nicola.michailow,andreas.festag,fettweis}
@ifn.et.tu-dresden.de

***Abstract*—The soft transition between generations of mobile communication systems is a desirable feature for telecommunication operators and device manufacturers. Looking to the past, clock compatibility between WCDMA and LTE allowed manufacturers to build inexpensive multi-standard devices. In this paper it is shown that GFDM, a candidate waveform for the 5G PHY layer, is able to use the LTE master clock and the same time-frequency structure as employed in today's generation of cellular systems. Two approaches for coexistence of 4G/5G waveforms are presented in the paper. The first GFDM setting is aligned with the LTE grid; in the other one GFDM acts as a secondary system to the primary LTE. The second approach introduces a new way of positioning subcarriers that further enhances the flexibility of GFDM. In addition, the paper also considers low latency aspects for autonomous and human controlled device communication in future application scenarios.**

***Keywords*—GFDM, LTE, 5G, clock compatibility, time-frequency grid, low latency.**

I. Introduction

The advent of mobile communication has caused a huge impact in modern life. The first generation has introduced the mobile voice communication, and telephony became personal. The second generation has included the Short Message Service, which turned to be an innovative way of personal communication. The third generation brought Internet browsing to our hands with throughput up to some Mbps. Now, we are seeing the deployment of the fourth generation based on Long Term Evolution [1], where data rates of up to 100 Mbps are being considered. High definition multimedia content can be generated and consumed by mobile devices allowing for unprecedent Quality of Experience (QoE).

Nevertheless, there are new applications arising whose requirements go beyond throughput. A completely new way of interaction with the virtual world, called Tactile Internet, could affect our society in several different ways [2], with applications in the area of e-health, entertainment, education, sports, robotics and smart grids, just to name some. Tactile Internet demands for very low latency in the order of 1 ms to provide an acceptable QoE. It is clear that the 25 ms latency provided by LTE is far beyond this requirement. Besides low latency, machine-to-machine (M2M) [3] communication will demand lower power transmission with a completely new data traffic profile. Sporadic transmission of short bursts will require random access to the communication channel without being perfectly synchronized with the base station in order to conserve energy. Low out-of-band (OOB) [4] emission is mandatory for minimizing the interference in surrounding channels in an opportunistic and fragmented spectrum allocation [5] approach. Several researches are ongoing to propose new waveforms that address the requirements for future mobile communication networks [6].

Generalized Frequency Division Multiplexing (GFDM) [7] [8] is an innovative multicarrier modulation scheme where the subcarriers are individually pulse-shaped in a block structure of M subsymbols and K subcarriers. Because all filter impulse responses are derived from a prototype baseband filter through time and frequency circular shifts, the GFDM signal is confined to MK samples. A single cyclic prefix (CP) for M subsymbols allows for simple frequency domain equalization. Although a new waveform might be necessary to deal with the new requirements of the fifth generation of mobile communication (5G), a completely disruptive approach is not interesting for operators. A compatible integration with the current generation would allow for a soft transition from one generation to the next, which is an interesting approach for those investing in telecommunication infrastructure. GFDM is a very flexible waveform, which covers Orthogonal Frequency Division Multiplexing (OFDM) [9] and Single Carrier Frequency Division Multiplexing (SC-FDM) [10] as corner cases, providing support for the two modulation schemes used in LTE [11].

Besides the compatibility of the modulation scheme, the new waveform should also be compatible with the LTE master clock rate. This requirement is important to allow manufacturers to re-use the already developed solutions for future networks, while new and more efficient solutions are being slowly introduced in the market. This concern was also observed when LTE was being conceived, once its master clock frequency is 8 times higher than the clock from the previous generation. It is very likely that next generation networks will employ a master clock that is an integer multiple of LTE's clock.

The aim of this paper is to demonstrate that GFDM can be synergetically used with the current LTE time-frequency grid, keeping the compatibility with most parameters of the current generation. GFDM can be designed to reduce the impact of the PHY layer in the overall system latency

978-1-4799-5863-4/14/$31.00

considering the resources available in the LTE frame. Two different approaches will be presented. The first one will use four resource blocks to fit three GFDM subcarriers, which are fully synchronized with the other LTE resource blocks. In the second approach, two LTE resource blocks will be used to fit one GFDM subcarrier. A guard band among the GFDM signal and the other resource blocks is introduced to allow for some asynchronicity between GFDM and LTE signals. Low interference with the LTE users is guaranteed by configuring GFDM with a low OOB emission [12]. This means that GFDM can use empty spectrum surrounding the LTE signal in an opportunistic and fragmented spectrum way, opening a new possibility of integration between 4G and 5G applications.

The remainder of this paper is organized as follows: Section II describes the GFDM principles and introduces a new approach to generate the subcarriers, where spectral separation is independent from the subsymbol separation. This feature is important to fit the wider GFDM subcarriers in the LTE time-frequency grid. Section III presents the GFDM parameters for both approaches analyzed in this paper. Section 4 shows the final conclusions and remarks.

II. GFDM Background

The basic block diagram of the GFDM system is depicted in Figure 1. The data bits are split in MN data streams and mapped in J-QAM data symbols, $d_{k,m}$. A GFDM symbol is composed of N subcarriers, each one carrying M data symbols in different time windows called subsymbol. The data symbols are oversampled by a factor MK and the resulting sequence is applied to transmit filters given by

$$g_{k,m}[n] = g[(n - mK) \mod MK] \exp\left(j2\pi \frac{k}{N} n\right), \quad (1)$$

where $k = 0, 1 \ldots, N-1$ is the frequency index, $m = 0, 1 \ldots, M-1$ is the subsymbol index, $n = 0, 1 \ldots, MK-1$ is the sample index, N is the subcarrier spacing factor and $g[n]$ is the prototype baseband filter impulse response. It is important to notice that all impulse responses used in the GFDM system are obtained by circular time and frequency shifts of the prototype impulse response. Therefore, the GFDM signal is self-contained in MK samples to which the CP is appended. Hence, the GFDM signal without the CP is given by

$$x[n] = \sum_{m=0}^{M-1} \sum_{k=0}^{N-1} d_{k,m} g_{k,m}[n]. \quad (2)$$

In previous GFDM proposals, the subcarrier spacing has been defined by the subsymbol distance, which means that $N = K$. However, GFDM is flexible and can accept different subcarrier spacings by making N independent from K. This is an important feature that will be explored in the next section to fit asynchronous GFDM subcarriers in the LTE time-frequency grid. Eq. (2) can be rewritten as [13]

$$\mathbf{x} = \mathbf{A}\mathbf{d}, \quad (3)$$

where $\mathbf{A}$ is the matrix containing all possible impulse responses $g_{k,m}[n]$ and $\mathbf{d}$ is the column vector with the data symbols $d_{k,m}$. Eq. (3) is an important representation of the modulation process and it can be used to explain different GFDM demodulation approaches, as will be shown later in this section.

Assuming that: i) the channel impulse response $h[n]$ is shorter than the CP length; ii) perfect time and frequency synchronization is accomplished and; iii) perfect channel state information is available on the receiver side, the signal after the CP removal is given by

$$y[n] = x[n] \circledast h[n] + w[n], \quad (4)$$

where $w[n]$ is the AWGN with standard deviation σ_w and $\circledast$ denotes circular convolution with respect to n and with periodicity MK. Frequency domain equalization (FDE) [14] can be performed, leading to

$$y_e[n] = \mathcal{F}^{-1}\left\{\frac{\mathcal{F}(y[n])}{\mathcal{F}(h[n])}\right\}, \quad (5)$$

where $\mathcal{F}$ is the discrete Fourier transform.

The GFDM demodulation process can be expressed as

$$\hat{\mathbf{d}} = \mathbf{B}\mathbf{y_e}, \quad (6)$$

where $\mathbf{B}$ is the demodulation matrix. Different linear approaches [15] can be used to recover the data symbols from the equalized GFDM symbol, as described below.

1) **Matched Filter Receiver (MFR)**: This receiver employs a bank of filters matched to the transmitter filters to recover the data symbols, maximizing the signal to noise ratio (SNR) per subcarrier. In this case, $\mathbf{B} = \mathbf{A}^{\mathrm{H}}$, where $(\cdot)^{\mathrm{H}}$ denotes Hermitian conjugate. The main disadvantage of the MFR is that intersymbol interference (ISI) and intercarrier interference (ICI) resulting from non-orthogonal pulse shapes can severely reduce its performance. Interference cancellation algorithms [16] can remove the interference and improve the performance of the system but entail an increment of the complexity on the receiver side.

2) **Zero-forcing Receiver (ZFR)**: This approach mitigates the ISI and ICI by using the inverse transmission matrix for receiving, i.e. $\mathbf{B} = \mathbf{A}^{-1}$. The ZFR collects information from the surrounding subcarriers in order to eliminate the interference. This procedure also gathers noise from outside the band of interest, which causes noise enhancement. The performance loss depends on the chosen $g[n]$ and it can be zero for orthogonal pulses, such as the Dirichlet [4].

3) **Minimum Mean Square Error Receiver (MMSER)**: The MMSER balances between MFR and ZFR. It acts as a MFR for low SNR, minimizing the effect of the noise in the demodulated data symbols. At high SNR, it acts as ZFR, mitigating the self generated interference. The price for the improved performance is an increased complexity on the receiver side. The demodulation matrix is given by $\mathbf{B} = (\mathbf{R}_w + \mathbf{A}^H\mathbf{H}^H\mathbf{H}\mathbf{A})^{-1}\mathbf{A}^H\mathbf{H}^H$, where $\mathbf{R}_w$ is the covariance matrix of the noise. Notice that MMSER equalizes the signal during the demodulation process. Hence, FDE is not required in this case.

III. Parameter Settings for GFDM

The evolution of mobile communication systems must take into account a soft transition between generations. The LTE system uses a master clock frequency that is 8 times higher than the one used in 3G, which has greatly simplified the development of hybrid devices, such as for 3G and 4G [17]. It

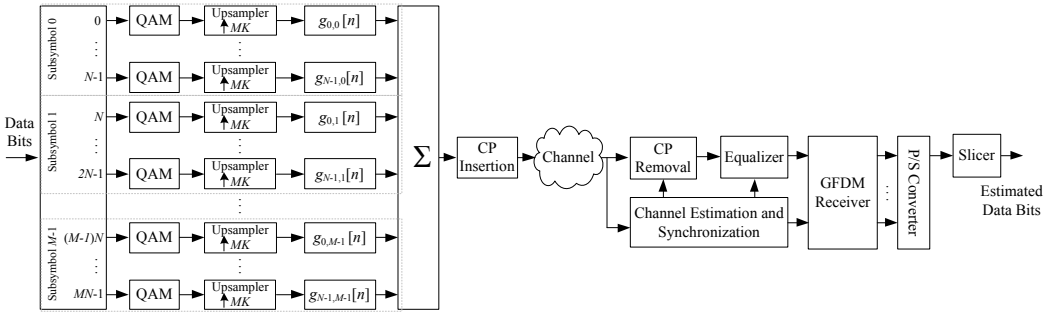

Fig. 1. Simplified block diagram of the GFDM system.

would be equally advantageous for manufacturers and telecommunication operators if the 5G standard would also be based on the LTE clock rate. In this section we show that GFDM signals can be integrated in the LTE time-frequency grid using the same clock rate of 30.72 MHz.

Moreover, low latency is an important feature for future wireless communication systems and GFDM can be designed to reduce the impact of the PHY layer in the overall system latency. The main approach is to reduce the GFDM symbol duration and add only a single CP for M subsymbols. The latter property is particularly important, because prefixing each subsymbol would actually increase the latency and reduce the spectral efficiency. The short subsymbol duration will lead to wider subcarriers that might suffer from frequency selective effects of the mobile multipath channel. But, because GFDM subcarriers have M times more samples in the frequency domain than LTE subcarriers, it is still possible to achieve acceptable symbol error rate performance. In this section we present two possible settings for GFDM to address two different scenarios. In the first one, there is only a GFDM signal which is configured to address low latency, using the master clock of LTE and in alignment with the LTE grid. The second approach allows the co-existence of a GFDM signal with current LTE systems.

To achieve a low latency, it is advantageous if each GFDM symbol can be demodulated independently. Hence, the channel estimation can not rely on the system frame structure and each symbol must carry all necessary information for single shot synchronization [12] and channel estimation. In consequence, similar or even more rigid pilot placements are required for low latency GFDM compared to the current LTE system. Nevertheless, throughput is not the main concern for time-critical applications and the increased overhead due a large amount of pilot subcarriers per GFDM symbol is acceptable in this scenario.

Although several improvements must be done also in the upper layers to achieve low latency, reducing the transmission time interval is a good step towards lower system latency and GFDM is a waveform flexible enough to address this aspect, as shown in the next subsections.

A. LTE structure

The parametrization presented in this paper considers a 20 MHz LTE system operating on frequency division duplex (FDD) mode as a reference. Table I shows the main parameters of the LTE system [1]. Other LTE signal bandwidths can be obtained by adjusting the number of active subcarriers.

TABLE I. LTE PARAMETERS FOR THE FDD MODE.

Parameter	Normal mode	Extended mode
Frame duration	10 ms or 307.200 samples	
Subframe duration	1 ms or 30.720 samples	
Slot duration	0.5 ms or 15.360 samples	
Subcarrier spacing	15 kHz	
Subcarrier bandwidth	15 kHz	
Sampling freq. (clock)	30.72 MHz	
# of subcarriers	2048	
# of active subcarriers	1200	
Resource block	12 subcarriers of one slot	
Number of OFDM per slot	7	6
CP length (samples)	First symbol: 160 Other symbols: 144	512

The LTE time-frequency grid is organized in resource blocks (RBs), each one having a bandwidth of 180 kHz bandwidth (12 subcarriers) and a duration of 0.5 ms (7 or 6 OFDM symbols for the normal and extended modes, respectively). A resource block is the basic quantity for resource allocation in LTE, which should be respected by a future 5G system. Figure 2 depicts the LTE resource block structure assuming normal operation mode.

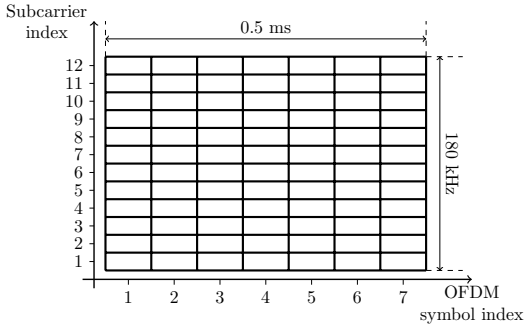

Fig. 2. Time-frequency structure of the LTE resource block on normal operation mode.

B. GFDM aligned with the LTE grid

In this case, the main objective is to integrate the GFDM signal in the time-frequency grid of the LTE system while enabling low latency applications. The duration of the GFDM symbol must be reduced to an integer fraction of the 1 ms subframe duration and a set of GFDM subcarriers must fit in an integer multiple of 180 kHz. Table II presents one possible set of GFDM parameters for this scenario.

TABLE II. GFDM CONFIGURATION ALIGNED WITH THE LTE GRID.

Parameter	Normal mode
Subframe duration	1 ms or 30.720 samples
GFDM symbol duration	66.67μs or 2048 samples
Subsymbol duration	4.17μs or 128 samples
Subcarrier spacing	240 kHz
Subcarrier bandwidth	240 kHz
Sampling freq. (clock)	30.72 MHz
Subcarrier spacing factor N	128
subsymbol spacing K	128
# active subcarriers N_{on}	75
# subsymbols per GFDM symbol M	15
# GFDM symbols per subframe	15
CP length	4.17μs or 128 samples
Prototype filter	Dirichlet

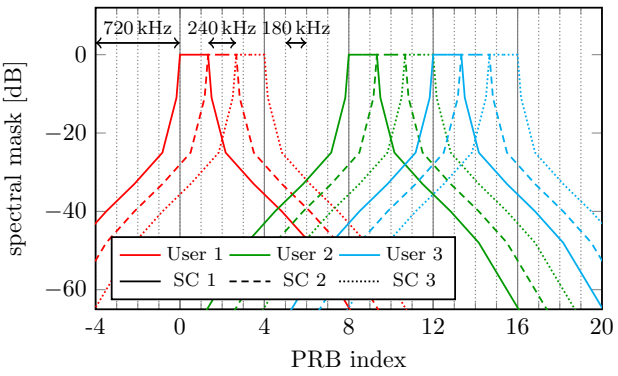

Fig. 3. GFDM frequency grid to match the LTE frame structure.

From Tables I and II, it can be seen that the proposed GFDM approach has the same subframe duration as the LTE grid. Nevertheless, the GFDM symbol duration is 7.5 times smaller than the equivalent slot duration of the LTE system. Assuming that the GFDM system is designed for independent demodulation of each symbol, it is possible to reduce the contribution of the PHY layer modulation to the latency by a factor of 15, compared with current LTE frame structure (LTE requires at least two slots of 0.5 ms to demodulate the user data). Of course, the total latency of the system also depends on a number of factors that cannot be addressed in this paper. However, Table II clearly shows that the GFDM PHY can contribute to the latency reduction while keeping the same time-frequency grid as the 4G system. Notice that three GFDM subcarriers occupy the bandwidth of four LTE resource blocks. This means that each GFDM subcarrier is 16 times wider than the LTE subcarriers. Because each GFDM subcarrier has $M = 15$ times more samples than an LTE subcarrier, the spectrum resolution of both systems is approximately the same. GFDM employs a slightly smaller CP length than LTE and it does not require a larger CP for the first GFDM symbol. The Dirichlet pulse makes the system orthogonal and, because the roll-off factor in the frequency domain is zero, the GFDM subcarriers do not overlap with the surrounding subcarriers outside of the used resource blocks. Therefore, the LTE time-frequency grid can be used to accommodate GFDM signaling as shown in Figure 3. Note that the conventional GFDM subcarrier spacing $N = K$ has been used here to match the LTE frame structure.

C. GFDM as a secondary system in the LTE grid

GFDM can also be configured to use two empty resource blocks, leaving a guard band to avoid interference in the surrounding resource blocks that are used to transmit the conventional LTE signal. In this case, the GFDM signal can be seen as a secondary signal that is used to explore vacant resource blocks for low latency applications. Table III shows the GFDM parameters for this approach.

TABLE III. PARAMETERS FOR ASYNCHRONOUS GFDM SIGNALLING.

Parameter	Normal mode
Subframe duration	1 ms or 30.720 samples
GFDM symbol duration	50 μs or 1536 samples
Subsymbol duration	3.125 μs or 96 samples
Subcarrier spacing	360 kHz
Subcarrier bandwidth	320 kHz
Sampling freq. (clock)	30.72 MHz
Subcarrier spacing factor N	256/3
Subsymbol spacing K	96
# active subcarriers N_{on}	half of available RBs
# subsymbols per GFDM symbol M	15
# GFDM symbols per subframe	20
CP length	3.125μs or 96 samples
Prototype filter	Dirichlet

A new approach to generate the GFDM signal must be introduced here in order to keep the subcarrier spacing compatible with the LTE time-frequency grid. The subcarrier bandwidth is 320 kHz, while the subcarrier spacing must be a multiple of 180 kHz (bandwidth of one RB). In order to achieve this frequency spacing, N must assume a value that differs from subsymbol spacing K. Nevertheless, N must be carefully chosen in order to guarantee that an integer number of subcarrier cycles is present within the duration of one GFDM frame, otherwise there will be phase jumps between the CP and the GFDM signal, leading to a strong out-of-band emission. The parametrization presented in Table III achieves this goal.

From Tables I and III it can be seen that the GFDM subcarriers are 21.33 times larger than LTE subcarriers in terms of bandwidth, while the GFDM symbol duration is 10 times smaller than the corresponding slot duration of the LTE system. Moreover, GFDM subcarrier resolution in the frequency domain is $M = 15$ times the resolution of the LTE subcarriers. The CP length has been shortened to 2/3 of the LTE CP length, which means that this approach is appropriate for small cell size (typically for diameter smaller than 4 km).

LTE equipment transmits system information periodically and even on empty resource blocks, which makes it difficult to use the approach proposed in Table III. One solution is to consider a LTE system operating in a spectrum hole that is larger than the system bandwidth, e.g., a 5 MHz signal being transmitted in the center of a 10 MHz band. Since the LTE grid is the same for any bandwidth configuration, with the only difference being the number of active subcarriers, the GFDM signal presented in Table III can be appended on the edges of the LTE signal, as depicted in Figure 4.

Notice that the low OOB emission of GFDM causes small interference in the LTE signal. However, the high OOB emissions of the LTE OFDM signal might be harmful for the GFDM signal [18]. The interaction of the LTE OOB with GFDM signals must be considered in order to specify the forward error control codes and other protective measures for the GFDM PHY layer.

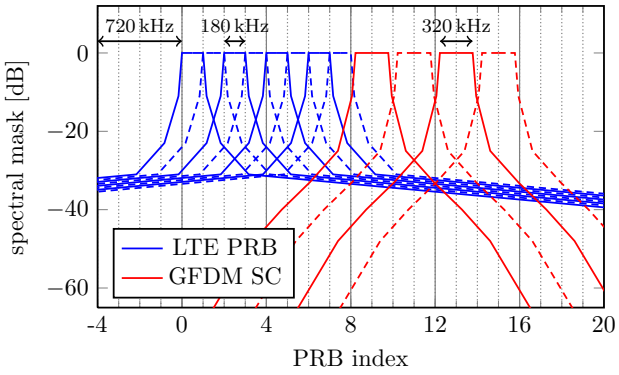

Fig. 4. GFDM as a secondary signal in the LTE time-frequency grid.

IV. Conclusions

Future 5G networks will have to deal with new challenges. New waveforms, more suitable for next generation applications, are being proposed and GFDM is a feasible candidate. Its flexibility covers OFDM and SC-FDM as corner cases and opens new possibilities for low OOB emissions and low latency applications. In this paper we have shown that GFDM can use the same clock rate as the current LTE system and can be configured to fit the same time-frequency grid. Two approaches have been explored considering the reduction of the PHY layer impact on the system latency. In the first one, a GFDM signal has been configured to perfectly fit the LTE grid, which can be used to reduce the latency by a factor of 15. In the second approach, a GFDM configuration is proposed to allow the coexistence of 5G and 4G signals, where the latency of the 5G signalling can be 10 times smaller than the current LTE system. Although the GFDM low OOB emission guarantees low interference in the LTE signals, the LTE OOB emission will affect the GFDM signal. Therefore, it is important to consider this interference when defining the error correction layer of the GFDM system. A new way to generate the GFDM signal has to be used in this case. Up to now, the spacing between adjacent GFDM subcarriers and their bandwidth have been equal. However, in the last approach, the spacing between the subcarriers must be larger than their bandwidth, which means that the subcarrier spacing factor is independent from the subsymbol spacing. This solution adds a new degree of freedom to GFDM in order to flexibly address the requirements of next generation of mobile communication networks. To design a complete approach for the coexistence of GFDM and LTE, further analysis regarding the signal structure and interference level must be carried out, but this paper has shown that the numerologie to adapt different configurations of GFDM to the LTE grid are possible, and this is an important first step.

Acknowledgment

The authors want to thank Vodafone Group R&D, Inatel and CNPq, Brasil; their support helped to create the results presented in this work.
This work has been performed in the framework of the FTP7 project ICT-318555 ”5GNOW” and ICT-258301 ”CREW”.

References

[1] F. Rezaei, M. Hempel, and H. Sharif, “LTE PHY Performance Analysis Under 3GPP Standards Parameters,” in *Proc. IEEE 16th International Workshop on Computer Aided Modeling and Design of Communication Links and Networks (CAMAD)*. Kyoto, Japan: IEEE, Jun. 2011, pp. 102–106.

[2] G. P. Fettweis, “The Tactile Internet: Applications and Challenges,” *IEEE Vehicular Technology Magazine*, vol. 9, no. 1, pp. 64–70, Mar. 2014.

[3] J. Kim, J. Lee, J. Kim, and J. Yun, “M2M Service Platforms: Survey, Issues, and Enabling Technologies,” *IEEE Communications Surveys & Tutorials*, vol. 16, no. 1, pp. 61–76, 2014.

[4] M. Matthé, N. Michailow, I. Gaspar, and G. Fettweis, “Influence of Pulse Shaping on Bit Error Rate Performance and Out of Band Radiation of Generalized Frequency Division Multiplexing,” in *Proc. Workshop on 5G Technologies (ICC’14 WS - 5G)*, Sydney, Australia, Jun. 2014, accepted for presentation.

[5] E. Hossain, *Dynamic Spectrum Access and Management in Cognitive Radio Networks*. Cambridge University Press, 2009.

[6] G. Wunder, P. Jung, M. Kasparick, T. Wild, F. Schaich, Y. Chen, S. Brink, I. Gaspar, N. Michailow, A. Festag, L. Mendes, N. Cassiau, D. Ktenas, M. Dryjanski, S. Pietrzyk, B. Eged, P. Vago, and F. Wiedmann, “5GNOW: Non-orthogonal, Asynchronous Waveforms for Future Mobile Applications,” *IEEE Communications Magazine*, vol. 52, no. 2, pp. 97–105, Feb. 2014.

[7] G. Fettweis, M. Krondorf, and S. Bittner, “GFDM – Generalized Frequency Division Multiplexing,” in *Proc. 69th IEEE Vehicular Technology Conference (VTC Spring’09)*, Barcelona, Spain, Apr. 2009.

[8] M. Matthé, L. Mendes, and G. Fettweis, “GFDM in a Gabor Transform Setting,” *accepted for publication in: Communications Letters, IEEE*, 2014.

[9] R. Chang, “High-Speed Multichannel Data Transmission with Bandlimited Orthogonal Signals,” *Bell Systems Technical Journal*, vol. 45, pp. 1775–1796, Dec. 1966.

[10] T. Kobayashi, A. Sano, A. Matsuura, Y. Miyamoto, and K. Ishihara, “Nonlinear Tolerant Spectrally-Efficient Transmission Using PDM 64-QAM Single Carrier FDM With Digital Pilot-Tone,” *Journal of Lightwave Technology*, vol. 30, no. 24, pp. 3805–3815, Dec. 2012.

[11] N. Michailow and G. Fettweis, “Low Peak-to-Average Power Ratio for Next Generation Cellular Systems with Generalized Frequency Division Multiplexing,” in *Proceedings International Symposium on Intelligent Signal Processing and Communications Systems (ISPACS’13)*, Naha, Okinawa, Japan, Nov. 2013, pp. 651–655.

[12] I. S. Gaspar, L. L. Mendes, N. Michailow, and G. Fettweis, “A Synchronization Technique for Generalized Frequency Division Multiplexing,” *EURASIP Journal on Advances in Signal Processing*, vol. 2014, no. 1, pp. 67–76, 2014.

[13] N. Michailow, I. Gaspar, S. Krone, M. Lentmaier, and G. Fettweis, “Generalized Frequency Division Multiplexing: Analysis of an Alternative Multi-Carrier Technique for Next Generation Cellular Systems,” in *Proceedings 9th International Symposium on Wireless Communication Systems (ISWCS’12)*, Paris, France, Aug. 2012, pp. 171–175.

[14] J. Ahn and H. Lee, “Frequency Domain Equalisation of OFDM Signals Over Frequency Nonselective Rayleigh Fading Channels,” *Electronics Letters*, vol. 29, no. 16, p. 1476, 1993.

[15] N. Michailow, S. Krone, M. Lentmaier, and G. Fettweis, “Bit Error Rate Performance of Generalized Frequency Division Multiplexing,” in *Proceedings 76th IEEE Vehicular Technology Conference (VTC Fall’12)*, Québec City, Canada, Sep. 2012, pp. 1–5.

[16] R. Datta, N. Michailow, M. Lentmaier, and G. Fettweis, “GFDM Interference Cancellation for Flexible Cognitive Radio PHY Design,” in *Proceedings 76th IEEE Vehicular Technology Conference (VTC Fall’12)*, Québec City, Canada, Sep. 2012, pp. 1–5.

[17] K. Ueda, T. Uozumi, R. Endo, T. Nakamura, T. Heima, and H. Sato, “A Digital PLL with Two-Step Closed-Locking for Multi-Mode/Multi-Band SAW-Less Transmitter,” in *Proc. IEEE Custom Integrated Circuits Conference*, San Jose, USA, Sep. 2012, pp. 1–4.

[18] N. Michailow, M. Lentmaier, P. Rost, and G. Fettweis, “Integration of a GFDM Secondary System in an OFDM Primary System,” in *Proc. Future Network & Mobile Summit*, Warsow, Poland, Jun. 2011.